Proceedings of the second INMM & ESARDA Joint Annual Meeting
May 22-26, 2023

Light-Extraction Characterization and Optimization for 2-D Photonic Crystals

S. R. Surani[a], P. E. Albert[b,c], F. Logoglu[a], D. E. Wolfe[b,c], and M. Flaska[a]

[a] *Ken and Mary Alice Lindquist Department of Nuclear Engineering*
[b] *Department of Materials Science and Engineering*
[c] *Applied Research Laboratory*
The Pennsylvania State University

Abstract

Inorganic scintillators are commonly used for various gamma-spectroscopy applications due to their relatively high light yield and good energy resolution. Because of their high refractive indices, inorganic scintillators often suffer from significant light losses due to total internal reflection. If the light collection at the scintillator-photosensor optical interface is improved, the energy resolution would also be improved, allowing for new applications for these scintillators. This project utilizes 2-D repetitive nanostructures, called photonic crystals, engineered onto the scintillator surface. Photonic crystals can enhance light collection from the scintillator through constructive light interference. The optimization simulations use Monte Carlo and deterministic models to simulate accurate light transport at micro- and nano-meter scales. Current simulations do not account for reflections at the scintillator-photosensor boundary and only represent the transmission for a single light pass. Future simulations will include multiple reflections. The latest simulations and experiments were performed using BGO inorganic scintillators. An optimized combination of a BGO scintillator coupled to 2-D Si_3N_4 photonic crystals improves the light transmission by more than 90% for a single light pass. Moreover, the optimized optical coupling is also being manufactured and will be analyzed using several gamma sources. The collected experimental data will validate and improve the existing simulation models. It is anticipated that the optimized, optically coupled nanostructures will lead to substantial enhancements in light collection and energy resolution.

Keywords: Photonic Crystals, Nanostructures, Inorganic Scintillators

1. Introduction

Inorganic scintillators are used for a wide range of gamma spectroscopy applications such as nuclear security, astronomy, and medicine [1]. These scintillators are preferred for their stable performance and high light yield [2]. Inorganic scintillators are often materials with a high refractive index, so despite their high light yield a large percentage of the light is reflected back into the scintillator due to total internal reflection, as described by Snell's Law [3]. A modified optical coupling between a high refractive index scintillator and a low refractive index photosensor could provide an optical bridge for trapped photons, allowing for more significant light extraction through constructive light interference. Photonic crystals (PHCs) are a periodic array of nanostructures with alternating high and low dielectric constants media [4]. This project uses PHCs to create an optical coupling that allows for more efficient light transmission through the scintillator material. An example of a PHC geometry is given in Figure 1. The PHC geometry itself, however, needs to be optimized for maximum light extraction.

This paper discusses modeling a gamma source, the scintillation process, and nano-meter scale light transport through the PHCs to provide a realistic simulation tool for optimizing the PHC structures. Earlier tests were done with a LYSO scintillator using the same method [5]. For this paper, a BGO ($Bi_4Ge_3O_{12}$) scintillator is modeled with silicon nitride (Si_3N_4) PHCs. BGO is non-hygroscopic and relatively inexpensive, making it suitable for the initial testing. BGO [6]also has a higher refractive index of 2.15 in comparison to LYSO [7], which has a refractive index of 1.81. Thus, we expect the optimized PHCs to improve BGO performance more substantially than LYSO. Future work will incorporate simulations with hygroscopic inorganic scintillators, such as sodium iodide (NaI) or lanthanum bromide ($LaBr_3$).

*Corresponding author. Tel.: +1 309 550 8445
Email address: srs6376@psu.edu (S. R. Surani)

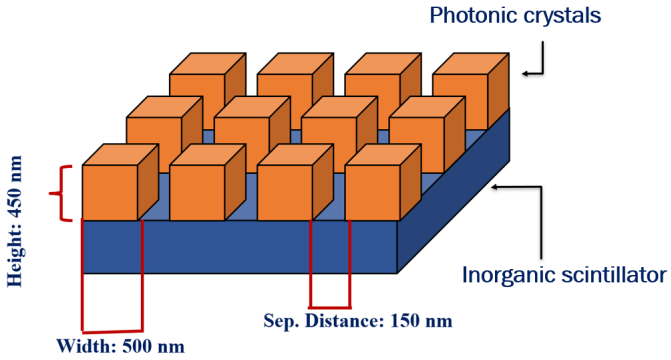

Figure 1: Schematic representation of a photonic crystal layer on a scintillator.

2. Methodology

The methodology for this project is shown in Figure 2. This project uses the Monte Carlo code Geant4 to simulate light production and transport in scintillator materials [8]. The Geant4 results were then used to build an input light source for the nanoscale simulations in OptiFDTD [9]. OptiFDTD is then used to generate and optimize the PHC geometry for the scintillator material. The last step of the process is manufacturing the optimized PHC geometry. The optimization step is closely tied to the manufacturing step to incorporate any manufacturing constraints and data from the experimental validation.

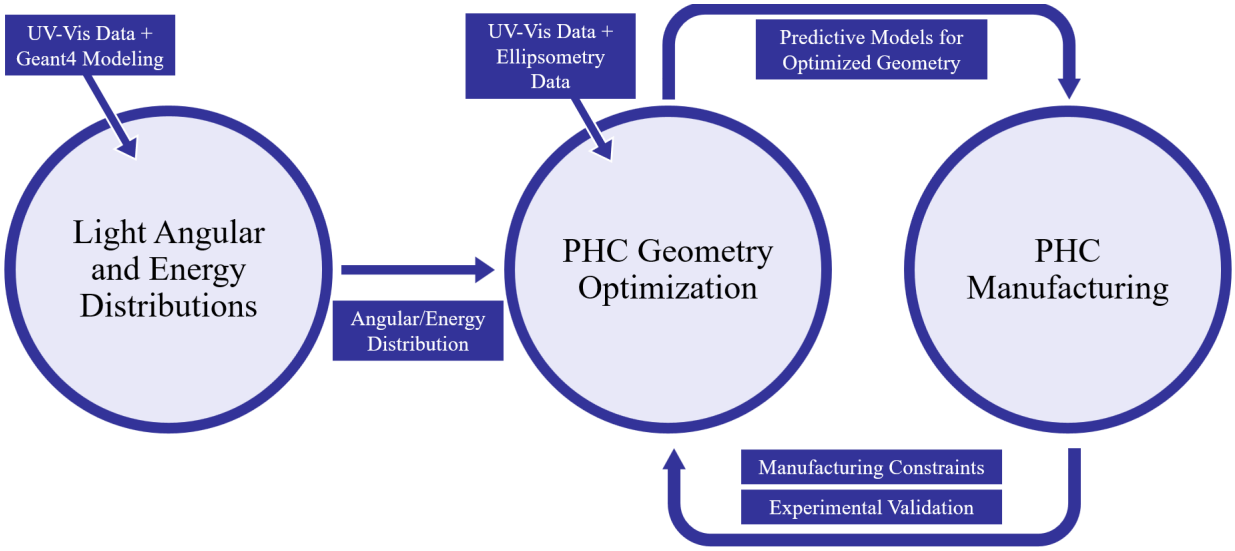

Figure 2: Flowchart for the methodology to optimize the PHCs.

2.1. Building the light source

The project utilizes two codes to simulate light transport across the scintillator and optimize the nanostructures. Geant4 is a Monte Carlo code that simulates light as particles called "optical photons." The code simulates the scintillation process within the scintillator that converts gamma radiation into photons. These photons are then tallied at the scintillator-photosensor boundary ,thereby providing a realistic light emission spectrum from the scintillator. A detailed view of the Geant4 simulation is shown in Figure 3.

We simulate a ^{137}Cs point source that produces optical photons within the scintillator consistent with the emission spectrum of the given scintillator. For BGO [6], the emission spectra are obtained from the manufacturer. The scintillation photons are simulated as an isotropic sources. Each photon reaching the scintillator photosensor boundary is tallied for its energy and angle, thereby obtaining angular and energy distributions for incoming light photons. The BGO scintillator is modeled with dimensions of 10 x 10 x 2.5 mm^3. The energy and angular distributions from Geant4 are used to build the input light source for OptiFDTD. At this point, these simulations only account for a single light pass through the scintillator-photosensor boundary. The light reflected and returned for a second pass is not calculated. Future simulations will include multiple reflections to further improve the overall light transmission.

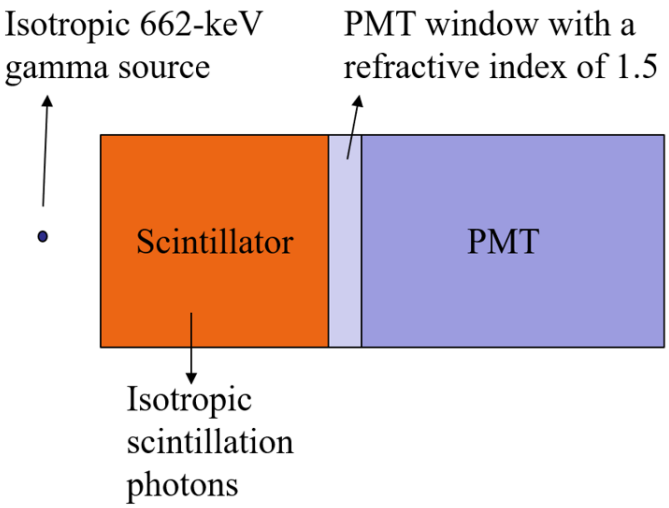

Figure 3: Geant4 simulation for the scintillation process.

OptiFDTD models light as electromagnetic waves allowing for a more complex treatment of light transport at the nanoscale level[9]. Material data for these simulations were obtained from ellipsometry measurements.

As shown in Figure 4, the computation region in OptiFDTD is divided into two regions: the reflected field region and the total field region. The regions are divided by the incident field, which only illuminates the total field region. This incident wave is generated as a planewave using a specific field distribution.

The angular distribution from Geant4 is approximated by rotating the planewave in 5-degree increments from -90 to 90 degrees. The energy spectrum can be approximated by using a Gaussian beam as expressed in Equation 1, where x_0 is the center position and T is the half width.

$$E(x) = A \cdot exp[-\frac{(x - x_0)^2}{2T^2}] \tag{1}$$

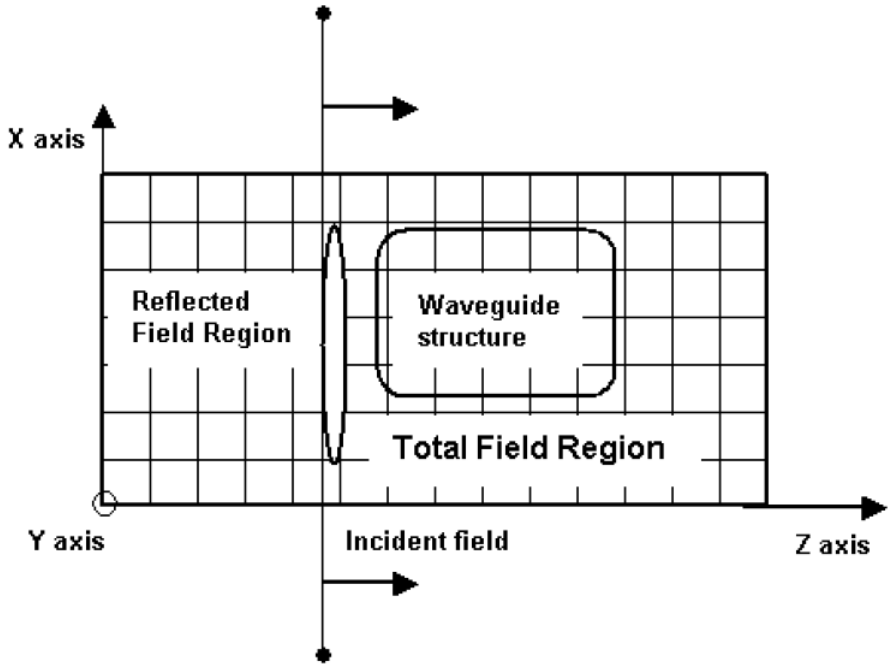

Figure 4: Input planewave in OptiFDTD.

2.2. *Photonic crystal optimization*

The PHC optimization simulations have many important variables, such as the crystals' shape, size, and spacing. We have considered a rectangular block structure for the preliminary tests, as shown in Figure 5. The PMT is modeled as a dielectric material with a refractive index of 1.5. The variables of interest are the height of the PHC (PHC z), the thickness of the PHC (PHC x), and the spacing between the PHCs (Gap). These variables are iterated from 0.1 um to 1 um for ten iterations each. The input source is located within the scintillator, and the transmission is calculated within the PMT.

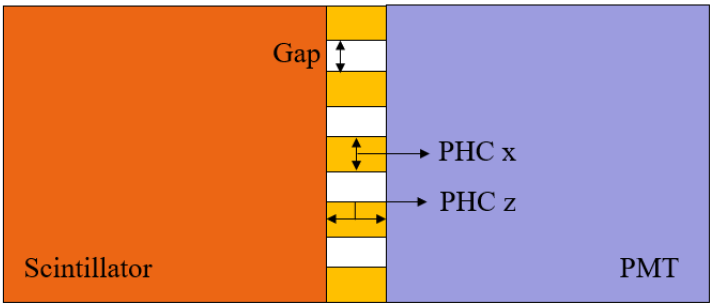

Figure 5: Schematic of photonic crystal simulation geometry in OptiFDTD.

3. Results

The energy and angular distribution of photons calculated from Geant4 is shown in Figure 6 for a 2.5-mm thick BGO crystal. BGO has a high refractive index and thus has significant total internal reflection. For a 2.5-mm BGO crystal, the total internal reflection for a single pass of light is 73%. On the other hand, for a 3-mm LYSO crystal, the total internal reflection for a single pass of light is 56%.

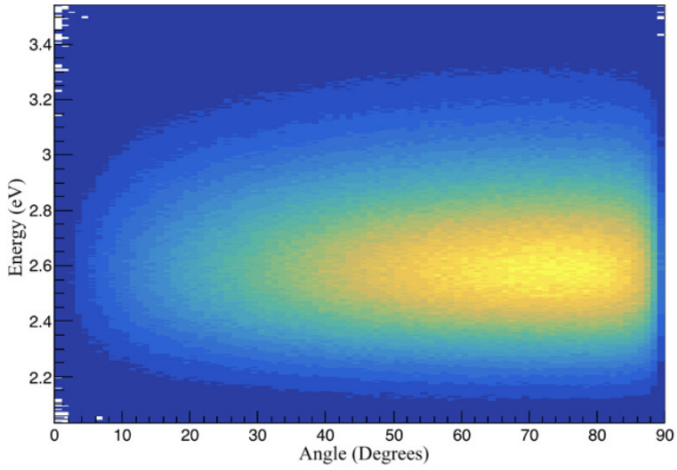

Figure 6: Angular and Energy distribution of photons for a 2.5-mm BGO scintillator.

The energy distribution is used to approximate the Gaussian spectrum in OptiFDTD. The BGO spectrum is approximated with a single Gaussian with a peak wavelength of 0.48 um as shown in Figure 7. The R-squared value between the two curves is calculated to be 0.99. This input source is then used for the optimization simulations.

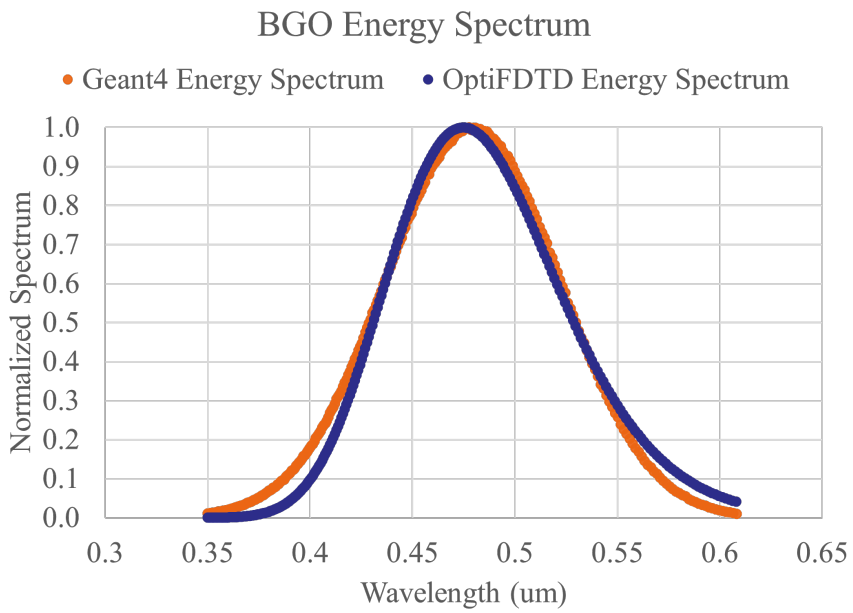

Figure 7: Energy spectrum approximation for BGO scintillator.

The optimization results for a single light pass are given for BGO in Figure 8. For a bare BGO, the transmission for a single light pass is 16.1%. The optimized geometry is determined to be 0.2 um Gap, 0.8 um PHC x, and 0.2 um PHC z with a single pass light transmission of 30.9%.

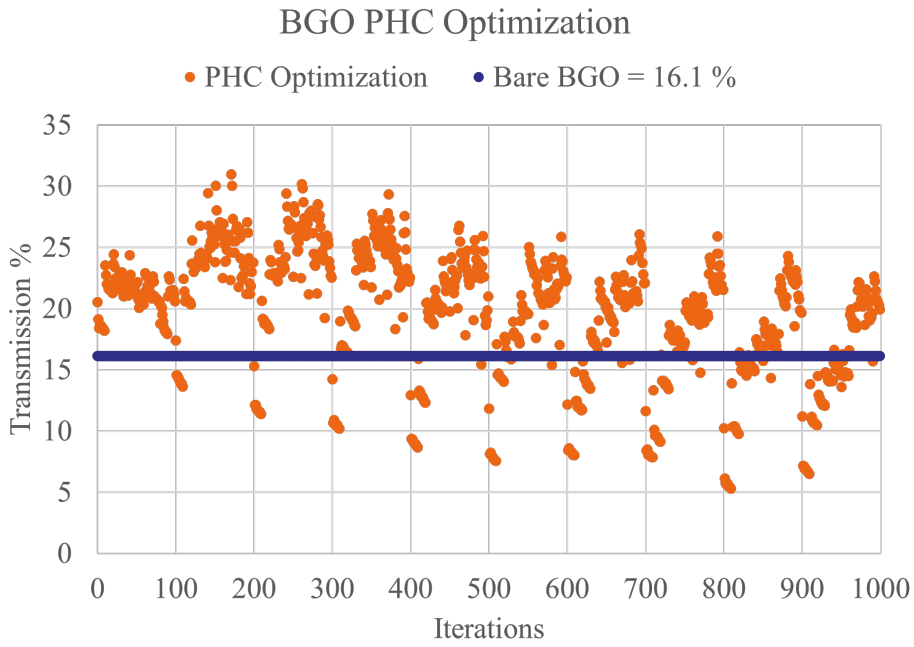

Figure 8: PHC optimization results for BGO.

The light transmission improvement is calculated as shown in Equation 2, where $T_{initial}$ is the transmission for the bare crystal and T_{final} is the transmission for the modified geometry with the PHCs.

$$Improvement\% = 100 \times \frac{T_{final} - T_{initial}}{T_{initial}} \tag{2}$$

BGO has an overall improvement in light transmission of 91.9%. The optimized BGO geometry is compared to

the optimized LYSO geometry [5] in Table 1. For both LYSO and BGO, we see similar optimized PHC geometry since both crystals have comparable light emission spectra. However, the percentage improvement in the transmission is greater for BGO since BGO has a higher refractive index, which results in larger TIR without PHCs.

Material	T_initial %	Gap	PHC x	PHC z	T_final %	Improvement %
LYSO	36.3	0.2 um	0.7 um	0.2 um	53.2	46.8
BGO	16.1	0.2 um	0.8 um	0.2 um	30.9	91.9

Table 1: PHC optimization results compared between LYSO and BGO.

4. Summary & Conclusions

The macro and nanoscale light transport simulations were performed by combining the Geant4 Monte Carlo code with the OptiFDTD deterministic code. The code integration required an approximation of the energy and angular light distributions from the Geant4 simulations to build the input light source for the OptiFDTD simulations. The current light source only takes into account a single pass of light. The optimization simulations for 2-D block structure PHCs were done for a BGO scintillator. We obtained an improvement of 91.9% for a 2.5-mm BGO scintillator. The optimized PHC geometry was compared for LYSO and BGO. BGO has a higher refractive index than LYSO and was expected to exhibit more improvement with the PHCs. Future simulations will incorporate 3-D geometries and different scintillator materials such as sodium iodide and lanthanum bromide.

The optimized PHC structures will be manufactured and characterized using various gamma sources to note the improvement in light output and energy resolution. Currently, we are conducting baseline experiments for a LYSO scintillator and working on the manufacturing process to construct these PHCs without deteriorating the optical properties of the LYSO scintillators.

Acknowledgements

This research is sponsored by the Defense Threat Reduction Agency (DTRA) of the Department of Defense (DOD) as part of the Interaction of Ionizing Radiation with Matter University Research Alliance (IIRM-URA) under contract number HDTRA1-20-2-0002.

References

[1] K. Vetter, R. Barnowksi, A. Haefner, T. H. Joshi, R. Pavlovsky, B. J. Quiter, Gamma-ray imaging for nuclear security and safety: Towards 3-d gamma-ray vision, Nuclear Instruments and Methods in Physics Research Section A: Accelerators, Spectrometers, Detectors and Associated Equipment 878 (2018) 159–168, radiation Imaging Techniques and Applications. doi:https://doi.org/10.1016/j.nima.2017.08.040.
URL https://www.sciencedirect.com/science/article/pii/S0168900217309269

[2] M. Reinhard, D. Prokopovich, H. Van der Gaast, D. Hill, Detection of illicit nuclear materials masked with other gamma-ray emitters, in: 2006 IEEE Nuclear Science Symposium Conference Record, Vol. 1, 2006, pp. 270–272. doi:10.1109/NSSMIC.2006.356153.

[3] F. Bryant, Snell's law of refraction, Physics Bulletin 9 (12) (1958) 317–317. doi:10.1088/0031-9112/9/12/004.
URL https://doi.org/10.1088/0031-9112/9/12/004

[4] A.Knapitsch, *et al.*, Results of photonic crystal enhanced light extraction on heavy inorganic scintillators, IEEE Transactions on Nuclear Science 59 (2012) 2334–2339. doi:10.1109/TNS.2012.2184556.

[5] S. Surani, P. Albert, F. Logoglu, P. Lauer, D. Wolfe, M. Flaska, 2-d nanoscale coating for optimized light extraction from inorganic scintillators, in: Proceedings of the 2022 IEEE Nuclear Science Symposium, Medical Imaging Conference and Room Temperature Semiconductor Detector Conference, 2022.

[6] Bgo scintillation material.
URL https://www.crystals.saint-gobain.com/radiation-detection-scintillators/crystal-scintillators/bgo-bismuth-germanate

[7] Lyso scintillation crystals.
URL https://www.crystals.saint-gobain.com/radiation-detection-scintillators/crystal-scintillators/lyso-scintillation-crystals

[8] S. Agostinelli, *et al.*, Geant4—a simulation toolkit, Nuclear Instruments and Methods in Physics Research Section A: Accelerators, Spectrometers, Detectors and Associated Equipment 506 (3) (2003) 250–303. doi:https://doi.org/10.1016/S0168-9002(03)01368-8.
URL https://www.sciencedirect.com/science/article/pii/S0168900203013688

[9] Optifdtd overview (Jun 2020).
URL https://optiwave.com/optifdtd-overview/